Proceedings of the Canadian Society for Mechanical Engineering International Congress
32nd Annual Conference of the Computational Fluid Dynamics Society of Canada
Canadian Society of Rheology Symposium
CSME-CFDSC-CSR 2025
May 25–28, 2025, Montréal, Québec, Canada

Tensile properties of ER70S-6 Thin Wall Geometry Built by Wire Arc Additive Manufacturing

Dat Vo, Jill Urbanic*, William Altenhof
Mechanical, Automotive and Materials Engineering, University of Windsor, Windsor, Canada
*jurbanic@uwindsor.ca

Abstract— Metal Additive Manufacturing (AM) technologies, particularly Wire Arc Additive Manufacturing (WAAM), have revolutionized the production of large-scale metallic components with complex geometries and tailored material properties. To adopt WAAM to the industrial application, it requires a high structural integrity, especially in aerospace, automotive, and shipbuilding industries. A thin wall ER70S-6 plate built using WAAM was evaluated through uniaxial tension tests, following ASTM E370-20 protocol, at strain rates ranging from 0.01 s^{-1} to 0.5 s^{-1}. The additive manufactured plate size was 250 mm x 140 mm x 3 mm. Specimens were extracted using a wire electrical discharge machine to cut to 20 specimens per plate. Tests were conducted with two surface conditions: raw and ground. Observations from this study noted that the error range of the test results was reduced when the specimens were ground. Importantly, it was observed that the material stiffness is significantly influenced by the surface conditions, a key finding of the research. A positive strain rate sensitivity was observed where the strength behaviour at 0.1 s^{-1} and 0.5 s^{-1} strain rates was found to be higher than findings from specimens tested at 0.01 s^{-1} strain rate. Findings from this research can be expanded to develop material models for the simulation of materials/structures developed using WAAM.

Keywords – Directed erergy depostion; Wire arc additive manufacturing; ER70S-6, Tensile; Thin-wall; As-built

I. INTRODUCTION

Additive manufacturing (AM) technologies have emerged as transformative solutions in the manufacturing industry, enabling the production of complex geometries and tailored material properties. Among these, Directed Energy Deposition (DED) has garnered significant attention for their scalability, cost-efficiency, and suitability for fabricating large-scale metallic components [1], [2]. One DED AM process is Wire Arc Additive Manufacturing (WAAM). The ER70S-6 wire filament is a low carbon steel widely used in welding applications. The use of ER70S-6 in has been shown as a promising candidate for industrial AM applications, particularly in sectors demanding high structural integrity, such as aerospace, automotive, and shipbuilding industries [3], [4], [5]. However, the mechanical performance of WAAM-fabricated ER70S-6 components under various conditions remains underexplored. The study of mechanical material performance in metals manufactured via WAAM is complicated by factors such as anisotropy, microstructural heterogeneity, and residual stresses, which arise from the inherently layer-by-layer deposition process. Tensile properties, especially when considering various construction approaches, are crucial for understanding how materials perform under different conditions such as quasi-static, impact, dynamic loading, or crash events.

Galloway and Nguyen have tested the tensile properties for ER70S-3, ER70S-6, and ER80S-Ni1 for two thick wall build configurations of 100 mm × 16 mm × 300 mm and 300 mm × 16 mm × 100 mm built using WAAM, as shown in Fig. 1. In both cases, these walls were built with four beads per layer. The ASTM E370-20 standard specimens were machined from the blocks [6]. The response of the ER70S-6 tensile mechanical tensile properties is close to its certified material test reports (CMTR); its elongation slightly increases while the yield and ultimate strength are similar to those of the CMTR. Also, they found that the material is slightly anisotropic, and the longitudinal coupon strength is higher than the transverse specimen strength by 10%[6].

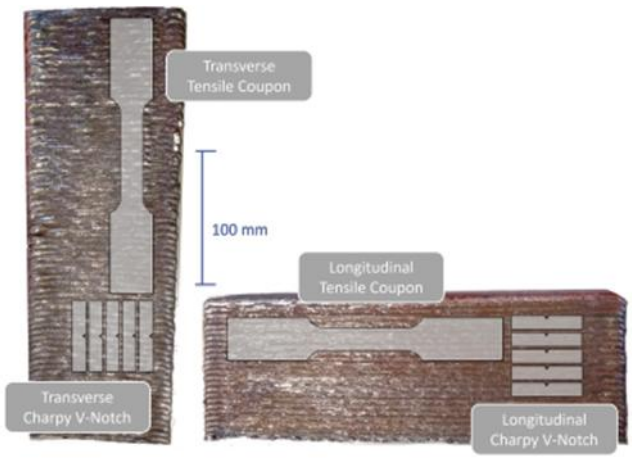

Figure 1. Galloway and Nguyen's two thick wall build configurations [6].

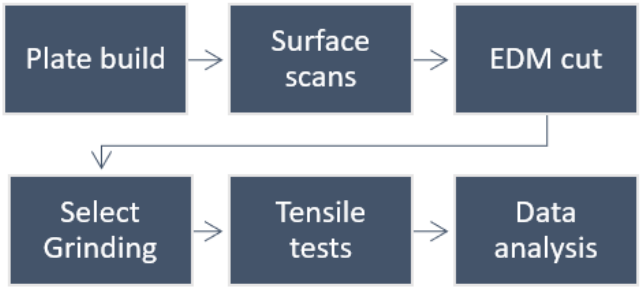

Figure 2. Research methodology process flow

Similarly, D.G. Andrade et al. have conducted tensile experiments for SS316LSi built using WAAM. Those wall plates had initial dimensions of 300 mm × 300 mm × 9 mm, built with three beads per layer [7]. Their research showed that machined tensile coupons always provide better mechanical strength than the as-built ones. There is an increase of 32% in yield strength, 24% in ultimate strength, and 61% in failure strength [7]. However, there has been no research on the characteristics of thinner wall build.

The present study aims to address this gap by evaluating the tensile layer-transverse properties of WAAM-fabricated ER70S-6 across a range of strain rates, from 0.01 s^{-1} to 0.5 s^{-1} with a thin wall geometry build configuration of 1 bead per layer. Through systematic experimentation and analysis, this research provides valuable insights for optimizing WAAM process parameters for high structural applications (design choice, structural integrity and safety), or finite element analysis.

II. Methodology

A systematic approach was conducted to ensure reproducible results, as shown in Fig. 2. An ER70S-6 thin-wall plate was fabricated using WAAM using a single bead stack deposition strategy, with the deposition head orthogonal to the build plate. Surface scans were performed to evaluate the initial surface roughness and distortion. Specimens were then cut using wire Electrical Discharge Machining (EDM) to maintain dimensional accuracy and minimize potential damage to their mechanical properties. Select post-cut specimens underwent an additional grinding process. Tensile tests were conducted to assess the mechanical properties under varying strain rates, and the resulting mechanical material data was analyzed.

(a) (b)

Figure 3. (a) The ER70S-6 WAAM setup and (b) the raw plate.

A. *Specimen preparation*

The base thin wall plate build size was 250 mm x 140 mm x 3 mm. The 3 mm width is the resultant width when using a single deposition bead configuration and zigzag deposition path. A Fanuc Arc Mate® 100iD 6-axis robot with a Lincoln Powerwave® R450 power source and wire feeder was used. The feedstock was ER70S-6 (B-G 49A 3 C S6), which is typically used in metal inert gas (MIG) applications. The chemical composition includes carbon (0.06% - 0.15%), manganese (1.40% - 1.85%), and silicon (0.80% - 1.15%). The shielding gas was 85% Argon + 15% CO_2. The arc voltage was 14.5 V, and the arc amperage was 43 A. The robot's travel speed is 508 mm/min, and the material wire feeding speed is 2540 mm/min. The plate was built on a mild steel foundation, and the cooling effect is through convection, to the surrounding atmosphere, and conduction with the mild steel foundation. The work cell and the base thin wall plate are shown in Fig. 3.

The tensile specimen geometry follows the ASTM E370-20 flat subsize standard with a gauge length of 32 mm and a width of 6.25 mm in Fig. 4(a). Raw (as built) and ground specimens were extracted from the same plate, as shown in Fig. 4(b) and Fig. 4(c). The specimens were cut with a wire electrical discharge machine to minimize the change in the characteristics of the material. The ground specimens were surface ground 0.05 mm per pass, until any surface defect(s) was/were not visually apparent.

The six (6) different testing conditions were considered in this study, which are shown in Table I. A base code QSX-Y-SZ is employed, where X is the strain rate in units s^{-1} (0.01, 0.1, or 0.5), Y is the specimen surface condition (R or G, standing for Raw or Ground, respectively), and Z is the specimen ID in the set. Different sample groups have different quantities of specimens. Due to material limitations, a total of twenty (20) specimens were tested sequentially to ensure the reliability and accuracy of the results.

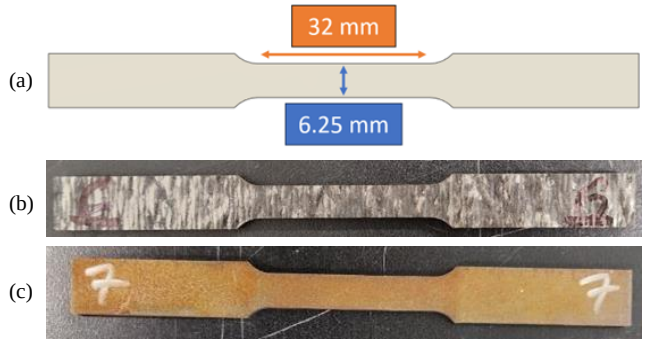

Figure 4. (a) ASTM E370-20 subsize specimen conditions, (b) raw and (c) ground

TABLE I. SPECIMEN GROUPS SUMMARY

Sample Group		Properties		
		Surface condition	*Strain rate (1/s)*	*Quantity*
	QS0.01-R	Raw	0.01	7
	QS0.1-R	Raw	0.1	4
	QS0.5-R	Raw	0.5	3
	QS0.01-G	Ground	0.01	4
	QS0.1-G	Ground	0.1	1
	QS0.5-G	Ground	0.5	1

B. *Mechanical characterization setup*

1) *Surface and thickness measurements*

A Keyence VR-5000 3D optical profiler was utilized to quantify the surface roughness. Data was obtained at 60 different points on the base plate's front and back. Those measured locations are approximately on the gauge of the specimens. To determine the specimen thickness, the cut specimen's images were taken to be analyzed with ImageJ. The average thickness of each specimen was calculated from 5 different locations along the gauge region.

2) *Uniaxial Tensile test*

Tensile testing was completed using a 50 kN MTS Criterion C43-504 universal test system. The mechanical extensometer used in the experimental efforts was a MTS 634.12F-24 10379295B, having a default gauge length of 25 mm. Along with the mechanical extensometer, a MTS video extensometer with 1.3 MP Allied Vision monochrome camera was used as a backup and for verification purposes.

III. RESULTS AND DISCUSSION

A. *Raw surface mapping*

Overall, the raw plate surface did not show warping or layer shifts. However, material dripping occurred on the edge, where the movement of the welding torch reversed its direction.

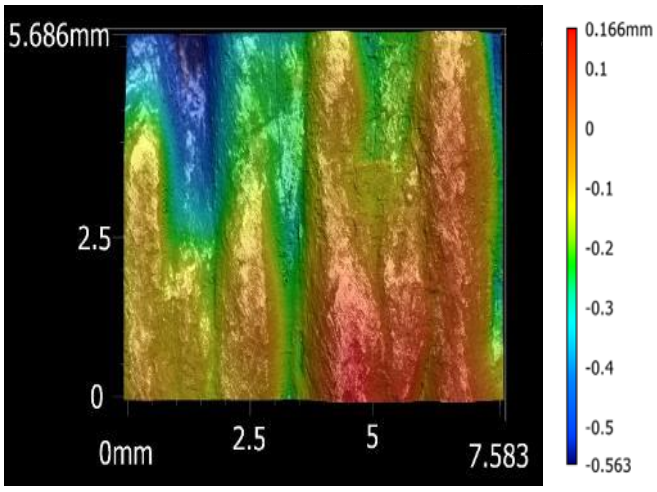

Figure 5. Roughness example at QS0.1-R-S2

TABLE II. ROUGHNESS SUMMARY OF THE RAW MATERIAL

	Sa (µm)	Sq (µm)	Sz (µm)	Sp (µm)	Sv (µm)
Mean	38.89	49.32	345.30	148.35	196.94
Standard Deviation	6.61	8.47	110.11	42.82	93.27
Min	26.03	33.25	214.75	81.66	106.11
Max	54.41	70.26	869.90	347.76	618.22

In Table II, the surface texture parameters are presented following the ISO 25178 standard. The average roughness values are reported as Sa = 38.89 µm (arithmetic mean height), Sq = 49.32 µm (root mean square height). The parameter Sz, representing the maximum height of the surface, shows significant variability with a standard deviation of 110.11 µm and values ranging from 214.75 µm to 869.90 µm. These Sz values indicate that the raw material surface has considerable unevenness, with some areas being relatively smoother and others exhibiting prominent peaks and valleys, which could affect the material performance. The peak (Sp) and valley (Sv) values are also provided, highlighting significant surface unevenness with maximum values of 347.76 µm and 618.22 µm, respectively. These results indicated considerable surface variability in the raw material condition. These values helped to estimate how much material needed to be removed with the surface grinder.

In Fig. 5, the valley depth measurement is -0.563 mm, while the peak reaches 0.166 mm, which creates a total surface variation of 0.729 mm gap. This significant height difference creates challenges for alignment during the grinding of the specimens, potentially leading to uneven material removal. Additionally, in the as-built condition, the valleys may act as geometrical stress concentrations, negatively affecting the mechanical performance of the specimens. This information helped to predict the worst scenario.

B. *Tensile testing mechanical properties*

1) *Baseline testing*

The QS0.01-R specimen group (Raw, 0.01 s^{-1}), which included seven specimens, provided observations for a baseline understanding of the surface to strength relationship. After that, the QS0.01-G specimen group was tested to compare and contrast, if any, to the strength characteristics of the raw surface specimen conditions.

The result in Fig.7(a) shows that with raw surface conditions, the specimens experienced a higher variation in yield strength range than specimens subjected to grinding, as presented in Fig.7(b). Variations in yield strength values of approximately 4% and 2% were discovered for the raw and ground surface conditions, respectively. The average engineering ultimate tensile strength of the QS0.01-R group and QS0.01-G group were similar, having an approximate value of 462 MPa. The QS0.01-R group experienced a shorter strain to failure compared to the QS0.01-G group by approximately 5%.

In Fig. 6(a), specimen QS0.01-R-S6 experienced an ultimate tensile strength greater than other specimens in the same group, at approximately 5% higher than the QS0.01-R's mean ultimate strength. Through inspection, QS0.01-R-S6 did not exhibit any visual critical defect, and its average cross-section area is 3% less than the average QS0.01-R gauge area. The flat and continuous surface condition most likely results in a higher strength capacity for this specimen. However, specimen QS0.01-R-S5 exhibited the lowest strain at failure compared to the rest of the specimens in the same group, and no significant visual surface defects were evident on this specimen.

Due to the minimal variation observed in the QS0.01-G group results and the inherent material limitations, the study prioritized evaluating the material in its as-is surface condition at higher strain rates.

2) Effect of Surface Condition (Raw vs Ground)

Interestingly, Fig. 7(a) shows a consistency of strength/strain of 3 specimens within the QS0.1-R grouping. Mechanical properties such as Young's modulus, yield strength, ultimate tensile strength and the strain to failure are consistent within these three specimens. In Fig. 7(b), mechanical material strength characteristics for specimens in the QS0.5-R group exhibit consistent findings.

Young's modulus was observed to be higher for the ground specimens compared to the raw surface finish condition, as shown in Fig. 9(c). This indicates that the surface grinding treatment improved material stiffness. A notably lower elastic modulus was observed for specimens with raw surface conditions at 0.1 s^{-1} and 0.5 s^{-1}. Material stiffness was observed to increase by 21% when the specimen surface was machined at these strain rates.

The yield strength and ultimate strength had minor variations for the raw and ground surface conditions. A 6% increase in these strength properties was observed when the samples were ground and tested at all different strain rates. However, surface grinding decreased the error ranges of both yield strength and ultimate strength from 13.1 MPa to 8.65 MPa and 11.87 MPa to 3.52 MPa, respectively.

Strain to failure was observed to significantly increase when a ground surface condition was implemented. Strain to failure increased by approximately 15% when the surface was ground. The enhancement in ductility is most likely associated with the elimination of geometric stress concentration at the weld beads in the raw condition. With surface grinding implemented, the standard deviation in strain to failure was also observed to decrease from 4.19% to 2.44%, as shown in Fig. 9(d).

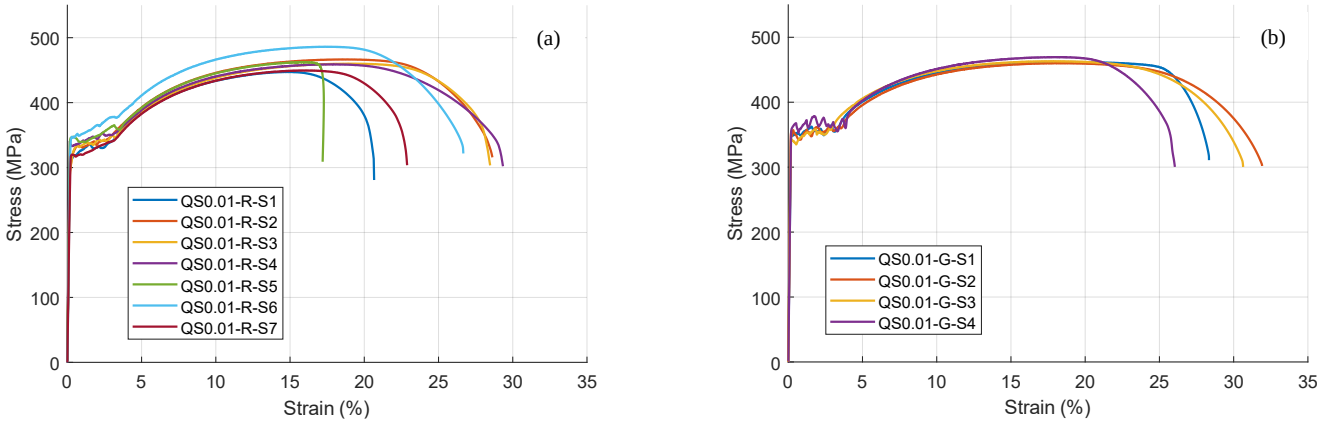

Figure 6. (a) Q0.01-Raw and (b) Q0.01-Ground engineering stress-strain responses

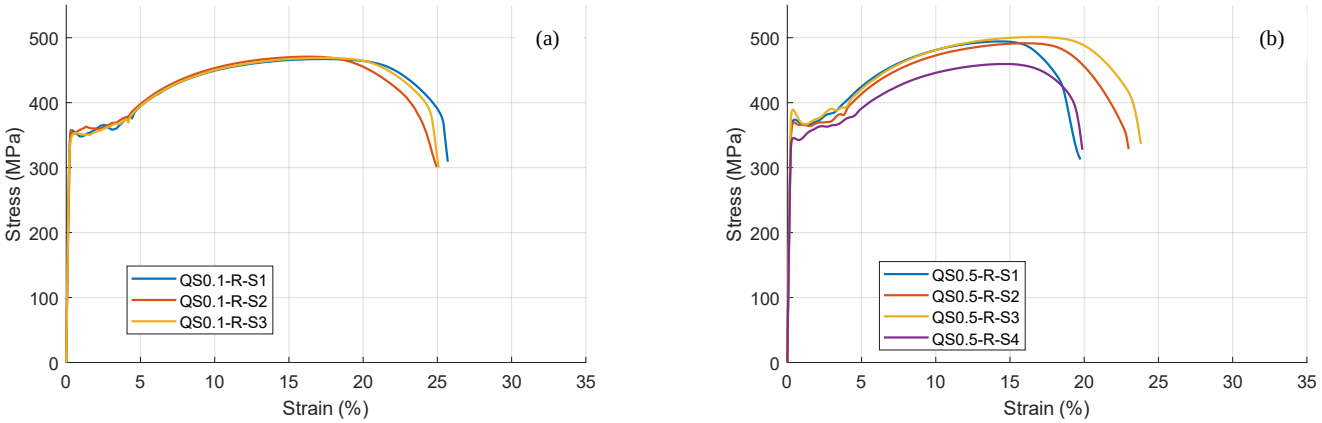

Figure 7. (a) Q0.1-Raw and (b) Q0.5-Raw engineering stress-strain responses.

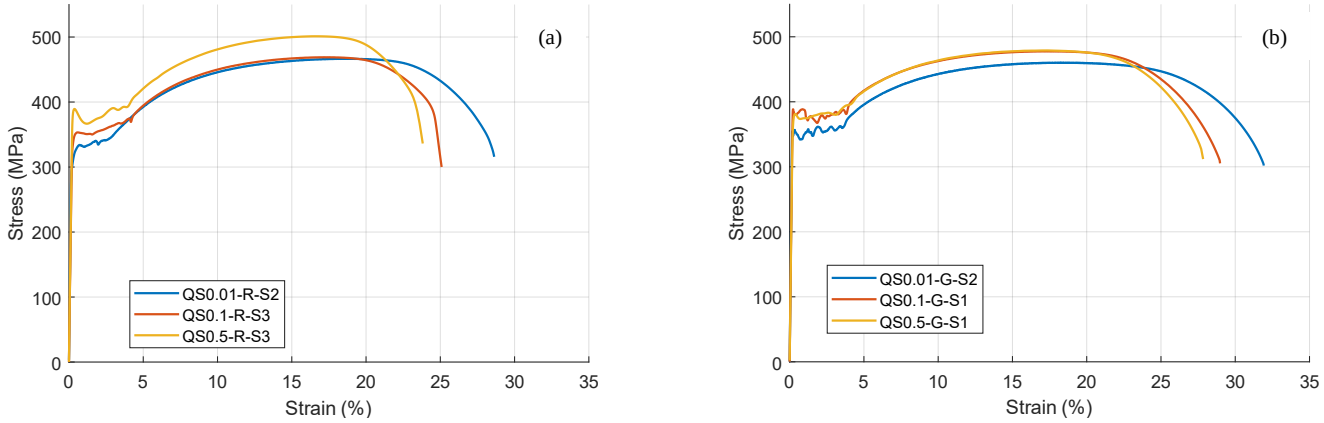

Figure 8. Different strain rates comparison between (a) raw specimen group and (b) ground specimen group.

3) Effect of Strain Rate on Mechanical Properties

Specimens within the QS0.1-G and the QS0.5-G grouping illustrated a positive strain rate sensitivity for the raw surface condition. However, variations in the tensile mechanical strength characteristics in the ground condition indicated only a minor rate sensitivity as the flow strength for the QS0.5-G was only slightly higher than QS0.1-G. Unfortunately, these findings are observed for conditions were only one specimen per group could be tested.

Overall, the yield strength and the ultimate strength of the material are higher at higher strain rates, which illustrates a positive rate sensitivity for this 3D printed material. Fig. 8 and Fig. 9(d) both illustrate the raw and ground specimens have a higher ductility when tested at a lower strain rate. The average strain reduction is approximately 3% when increasing the strain rate from 0.01 s^{-1} to 0.5 s^{-1}.

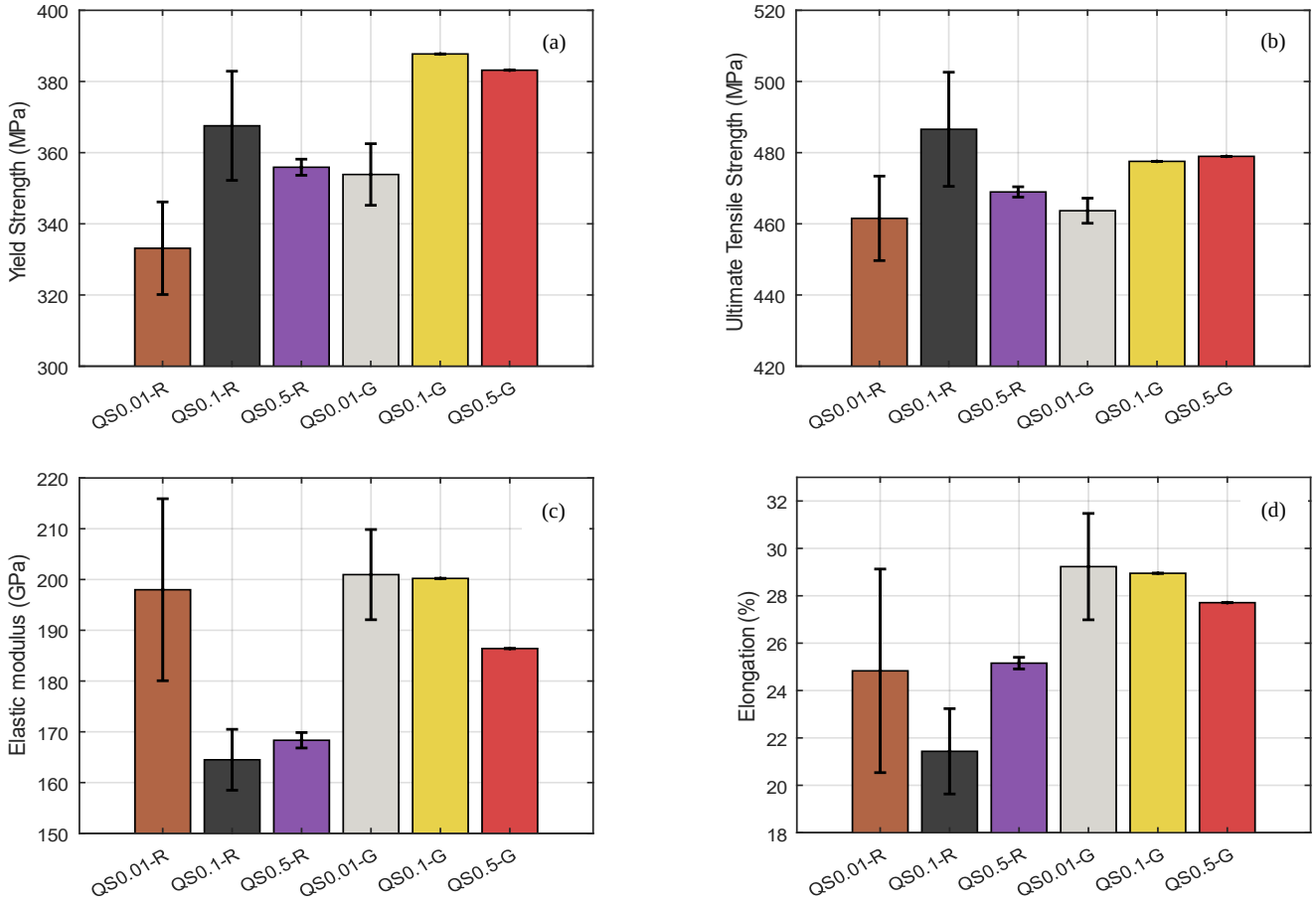

Figure 9. Summary of tension characteristics: (a) yield strength, (b) ultimate tensile strength, (c) elastic modulus and (d) strain to failure.

There was a 9% rise in the average strength in specimens with the raw surface conditioning specimen group, when the strain rate increased from 0.01 s^{-1} to 0.5 s^{-1}. Meanwhile, the ground specimen group only experienced approximately 20 MPa increase in strength at the 0.5 s^{-1} strain rate compared to 0.01 s^{-1}. The ultimate strength of QS0.1-G-S1 was not different to the QS0.5-G-S1, although the strain rate is five times higher. The QS0.5-G-S1 specimen experienced a lower strain compared to the QS0.1-G-S1 specimen by 1%.

4) Thin-wall vs thick-wall build comparison

Compared with Galloway and Nguyen's experimental results, there is a reduction in ER70S-6 material strength when building with a 3 mm single bead wall configuration compared to the 16 mm thick-wall build [6]. In Fig. 9, the average yield strength and ultimate tensile strength of the QS0.01-G are 354 MPa and 464 MPa respectively, while the thick-wall build with the same orientation from Galloway and Nguyen's experiment shows 395 MPa yield strength and 512 MPa ultimate tensile strength [6]. That means there is a 10% strength deduction when built with single bead/zigzag build configuration. The thin-wall configuration elongation is also lower by 2% of the total strain compared to thick-wall build.

5) Nonuniform strain along the raw specimen

As shown in Fig. 10, the raw specimen experienced a nonuniform strain along its gauge length. At 25% of the test process, the upper-middle regime started to experience localized deformation (highlighted in the red dash rectangle). However, a shift in the localized deformation region occurred at approximately 50% of the test, where a localized deformation region lower in the specimen was observed. Finally, the specimen failed at the 1st defined region of localized deformation. Depending on the nonuniform cross-section area and any discontinuities of geometry within the gauge region, the localized deformation, corresponding to regions of high stress, may peak at different regions and may also be associated with interior material microcracks.

IV. Summary

The tensile mechanical strength behaviour of 3D printed ER70S-6 thin plates were evaluated at quasi-static strain rates through uniaxial tension testing. The quasi-static uniaxial tension tests included a study of specimen surface condition and a variation in strain rate. The key findings of this investigation are as follows:

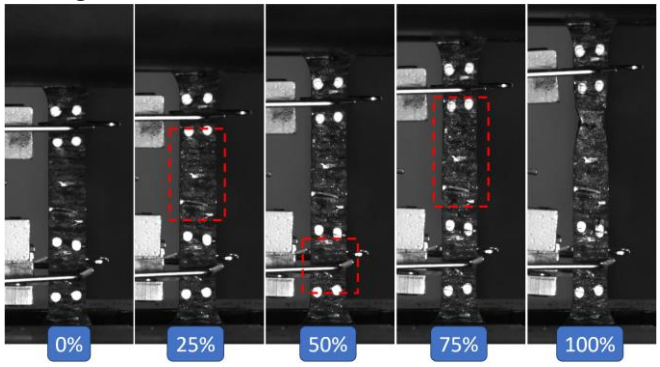

Figure 10. QS0.01-R-S4 ununiform strain during testing process example

1. Both yield strength and ultimate tensile strength increase with the strain rate.
2. The surface preparation has a more pronounced effect at lower strain rates.
3. Surface ground specimens exhibited higher mechanical strength characteristics compared to raw specimens.
4. A 10% reduction of strength and elongation for the ER70S-6 deposited in one 3 mm bead, exploiting a zigzag building strategy, compared to a thick-wall 16 mm build.

Overall, this research has found that the ER70S-6 material strength decreases when a thin-wall 3D print build strategy is implemented. Findings from this study also provide useful mechanical material strength data to design parts with this manufacturing process.

Acknowledgment

Special thanks to Professor Tam Nguyen and Professor Jim Galloway at Conestoga College.

References

[1] RAMLAB, "What is DED? - DED fully explained by the RAMLAB knowledge hub," RAMLAB. Accessed: Sep. 01, 2024. [Online]. Available: https://www.ramlab.com/resources/ded-101/

[2] "Wire Arc Additive Manufacturing (WAAM)." Accessed: Sep. 01, 2024. [Online]. Available: https://www.twi-global.com/technical-knowledge/job-knowledge/arc-based-additive-manufacturing-137.aspx

[3] "Metal Additive Manufacturing Market Size, Share, Report 2023-2032." Accessed: Aug. 16, 2024. [Online]. Available: https://www.precedenceresearch.com/metal-additive-manufacturing-market

[4] "Metal Additive Manufacturing Market Size, Trends, Growth And Forecast 2024-2033." Accessed: Aug. 16, 2024. [Online]. Available: https://www.thebusinessresearchcompany.com/report/metal-additive-manufacturing-global-market-report

[5] "WELD Magazine | SOUDURE Magazine - Investigation And Qualification Testing Of GMAW Wire Arc Additively Manufactured Structural Steel Components." Accessed: Sep. 01, 2024. [Online]. Available: https://www.weldmagazine.com/weldmagazine/library/item/weld-spring2022/3995508/

[6] "WELD Magazine | SOUDURE Magazine - Investigation And Qualification Testing Of GMAW Wire Arc Additively Manufactured Structural Steel Components." Accessed: Jan. 14, 2025. [Online]. Available: https://www.weldmagazine.com/weldmagazine/library/item/weld-spring2022/3995508/

[7] D. G. Andrade, T. Tankova, C. Zhu, R. Branco, L. S. Da Silva, and D. M. Rodrigues, "Mechanical properties of 3D printed CMT-WAAM 316 LSi stainless steel walls," *J. Constr. Steel Res.*, vol. 215, p. 108527, Apr. 2024, doi: 10.1016/j.jcsr.2024.108527.